The electrocatalytic oxidation of ethanol studied on a molecular scale

Lai, S.S.S.

CHAPTER 3

ETHANOL AND ACETALDEHYDE ELECTRO-OXIDATION ON PLATINUM SINGLE-CRYSTAL ELECTRODES IN ACIDIC MEDIA

The electrochemical oxidation of ethanol and acetaldehyde in sulfuric acid and perchloric acid were studied at Pt (111), Pt (110), and a number of Pt [n(111)×(111)] single-crystal electrodes. The oxidation of ethanol shows a marked dependence on the surface structure, roughly increasing as the surface step density increases. The oxidation of acetaldehyde shows a reversed correlation, the activity decreasing with increasing step density. Based on the results obtained here and reported earlier in electrochemical and ultra-high vacuum literature, a detailed reaction scheme for the ethanol oxidation mechanism is suggested.

The contents of this chapter have been published: S. C. S. Lai and M. T. M. Koper, *Faraday Discuss.*, **2008**, *140*, 399-416.

3.1 Introduction

The electrochemical oxidation of ethanol on platinum electrodes has been a subject of increasing interest [1-5]. From an environmental point of view, ethanol, which can be produced by the fermentation of bio-mass, is often mentioned as one of the main candidates for use in low temperature fuel cells [6]. Apart from practical advantages, such as the ease in storage and transportation and its non-toxicity, ethanol has a high theoretical energy content of 8.0 kWh kg^{-1}, corresponding to 12 electrons per molecule for its total oxidation to carbon dioxide [3]. Therefore, the main challenge in the electrochemical oxidation of ethanol is to achieve total conversion at a low overpotential. The main problem in achieving an efficient conversion is that the ethanol oxidation reaction occurs through different reaction pathways. In some pathways, large amounts of partially oxidized products are produced due to the difficulty in breaking the C-C bond. These partially oxidized products, which include acetaldehyde [4, 7-9] and acetic acid (or acetate) [1, 2, 4, 7, 9], do not only decrease the total efficiency of the system, but are also unwanted due to their polluting nature. In other pathways, strongly adsorbed species such as carbon monoxide [4, 7, 9] and carbohydrate (CH_x) fragments [5, 10] are formed, which poison the platinum surface.

Despite the great number of papers dedicated to the electrochemical oxidation of ethanol, there are still a significant number of issues in the understanding in the mechanism of ethanol electro-oxidation. One of the main mechanistic issues lies in determining in which pathways carbon dioxide is produced, and therefore, in determining the molecular species in which the carbon-carbon bond is broken as well as the electrochemical nature of the resulting decomposition products. In this context, the present study will employ a series of well-defined platinum single-crystal electrodes to investigate the effect of surface structure on the oxidation of ethanol and acetaldehyde. We will compare our results to previous results, especially in relation to ethanol decomposition on similar (stepped) Pt single-crystals in ultra-high vacuum (UHV). In the discussion section, we will propose a reaction scheme that is able to rationalize most of the results obtained here and in previous work.

3.2 Experimental

Electrochemical measurements were carried out in a conventional single-compartment three-electrode glass cell. The cell and all other glassware were cleaned by boiling in 1:1 mixture of concentrated nitric acid and sulfuric acid followed by repeated boiling with ultra-pure water (Millipore MilliQ A10 gradient, 18.2 MΩ cm, 2 - 4 ppb total organic content) before each experiment.

In all experiments, a platinum wire was used as counter electrode. For experiments with H_2SO_4 as electrolyte, a mercury-mercury sulfate electrode (MMSE: $Hg/Hg_2SO_4/K_2SO_4$) was employed as a reference electrode, while a reversible hydrogen electrode (RHE) was used for measurements in experiments with $HClO_4$ as electrolyte. In all cases, the reference electrode was connected via a Luggin capillary. All potentials reported here have been converted to the RHE scale in the same electrolyte. The working electrodes used in this study for the voltammetric measurements were platinum bead-type single-crystal electrodes of Pt [n(111)×(111)] (or, equivalently, Pt [(n-1)(111)×(110)]) orientation. The surfaces studied were Pt (15 15 14) with n = 30, Pt (554) with n = 10, Pt (553) with n = 5 and the limiting cases Pt (111) and Pt (110), which were prepared according to Clavilier's method [12]. Both the terrace width n and the step density (defined as $\theta_{step} = 1 / (n - {}^2/_3)$) will be used in this study as a quantitative measure for the amount of steps [13]. Prior to each experiment, the electrodes were flame-annealed and cooled down to room temperature in an argon (Air Products, "BIP Plus", 6.6) - hydrogen mixture (Air Products, "Ultrapure Plus", 6.0) (*ca.* 3:1), after which they were transferred to the electrochemical cell under the protection of a droplet of deoxygenated ultra-pure water [14].

The supporting electrolytes, 0.5 M H_2SO_4 and 0.1 M $HClO_4$, were prepared with concentrated sulfuric or perchloric acid (Merck, "Suprapur") and ultra-pure water. Electrolytes containing ethanol, acetaldehyde or acetic acid consisted of the blank electrolyte and 0.5 M ethanol (Merck, pro analyse), 0.1 M acetaldehyde (Sigma-Aldrich, "ReagentPlus") or 0.1 M acetic acid (Sigma-Aldrich, "ReagentPlus"), respectively. Argon (Air Products, "BIP Plus", 6.6) was used to deoxygenate all solutions. It should be noted that the concentration of 0.5 M ethanol corresponds to a value that would be a sensible concentration

in a real fuel cell. According to the work of Camara and Iwasita, this ethanol concentration leads to acetaldehyde as the primary reaction product. Similarly, the main reaction product of acetaldehyde oxidation in the concentrations employed in this study is acetic acid [11]. Voltammetric measurements were performed at room temperature (20° C) using a computer-controlled Autolab PGSTAT 12 potentiostat (Ecochemie).

3.3 Results and discussion

3.3.1 Ethanol

Continuous oxidation

Figure 3.1 shows typical voltammograms obtained for the electro-oxidation of 0.5 M ethanol on Pt (111), Pt (110) and on the stepped surfaces Pt (15 15 14), Pt (554) and Pt (553) in 0.5 M H_2SO_4, sweeping initially positive from 0.07 V at 10 mV s^{-1}. The positive potential limits were chosen in each case before the onset of surface oxidation to avoid surface disordering due to irreversible oxide formation. A number of general features can be observed on all electrode surfaces: in the positive scan, the current is negligible up to 0.4 V. At this potential, a pronounced increase in the current occurs, forming a small shoulder at ~0.5 V followed by a large peak with a maximum between 0.6 and 0.8 V. During the return scan, the current increases again to produce a single peak. In the case of Pt (111), a small but reproducible increase in the current can also be observed at 0.44 V. The position of this current increase corresponds strongly with the location of the so-called Pt (111)-butterfly [15], which is commonly ascribed to the order-disorder transition of the (bi-)sulfate adlayer [15, 16]. In addition, similar to the Pt (111)-butterfly, this feature was found to be very sensitive to the long-range crystalline order of the electrode, being, for example, more pronounced on Pt (111) cooled in an H_2/Ar mixture after flame annealing and disappearing entirely on a Pt (111) electrode cooled in air after flame annealing, even though the blank voltammetry showed only small differences [14]. Therefore, we attribute this feature to the increased availability of surface sites due to a sharp decrease of the coverage of the strongly adsorbing (bi-)sulfate anion.

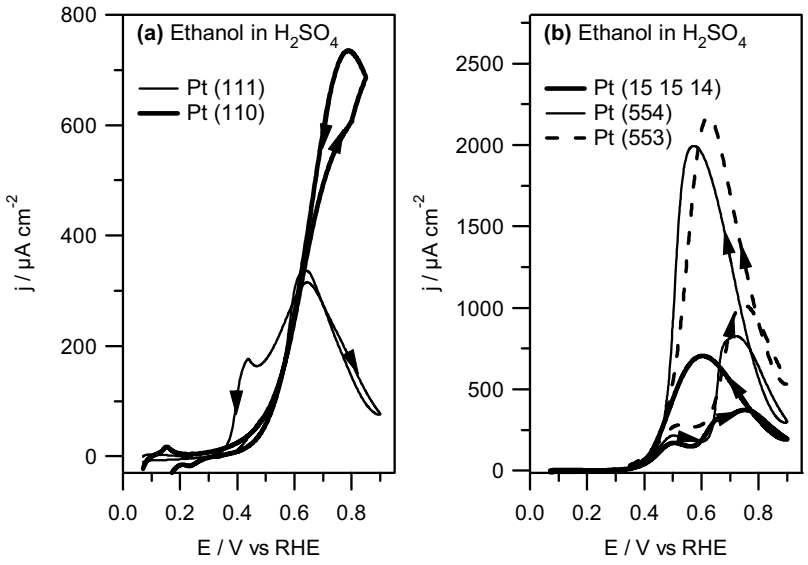

Figure 3.1: *Cyclic voltammograms for the electro-oxidation of 0.5 M ethanol in 0.5 M H_2SO_4 on (a) Pt (111) and Pt (110) and (b) Pt (15 15 14), Pt (554) and Pt (553), respectively. All voltammograms were recorded at a scan rate of 10 mV s^{-1}. Arrows indicate the scan directions.*

By comparing the CVs of the different surfaces in Figure 3.1, it can be observed that upon increasing the step density by going from Pt (111) to Pt (15 15 14), the maximum activity towards ethanol oxidation roughly doubles, while a further increase in the step density to Pt (554) yields another increase in the maximum current by a factor of three. As the step density is increased further from Pt (554) to Pt (553), the maximum activity increases slightly, before dropping by a factor of three in passing from Pt (553) to Pt (110). These results indicate that, similar to the oxidation of CO [17, 18] and methanol [19], defects enhance the ethanol oxidation rate in sulfuric acid. There are, however, significant differences in the quantitative effect of step density. In the case of CO, the oxidation rate constant was found to be linearly dependent on step density over the entire range of step densities [18]. In the present study, the peak current density appears to show a rough linear dependence for terraces of over 10 atoms wide (Figure 3.3a). This is also the range in which the overpotential required for the peak activity is decreasing with step density (Figure 3.3b). For narrower terraces,

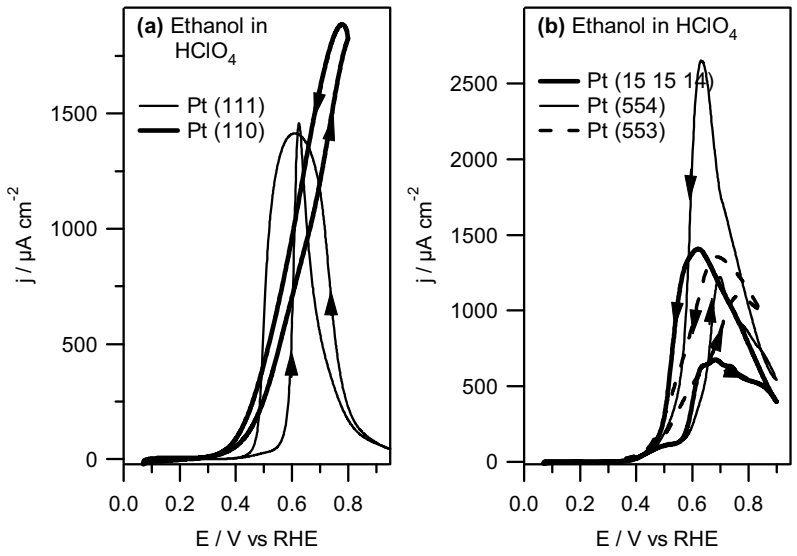

Figure 3.2: *Cyclic voltammograms for the electro-oxidation of 0.5 M ethanol in 0.5 M $HClO_4$ on (a) Pt (111) and Pt (110) and (b) Pt (15 15 14), Pt (554) and Pt (553), respectively. All voltammograms were recorded at a scan rate of 10 mV s^{-1}. Arrows indicate the scan directions.*

this trend is observed to reverse; it is especially noteworthy that the oxidation activity of Pt (110) in sulfuric acid is below that of Pt (554) and Pt (553), both in terms of the peak current density as well as in the location of the peak potential. This effect was also found in the case of methanol oxidation on the same surfaces [19], indicating that the oxidation of ethanol requires some combination of steps and terrace sites. Considering the deviation from the linear trend when the terrace width is decreased below 10 atoms, it is likely that there is an optimum terrace width for ethanol oxidation.

To study the effects of anion adsorption, the same experiments were also conducted using 0.1 M $HClO_4$ as supporting electrolyte. Typical voltammograms for the oxidation of ethanol on Pt [*n*(111)×(111)] type electrodes in perchloric acid are shown in Figure 3.2. Similar to methanol electro-oxidation, the shape of the voltammetric profiles does not differ significantly in both acidic media [19]. Furthermore, there were no significant

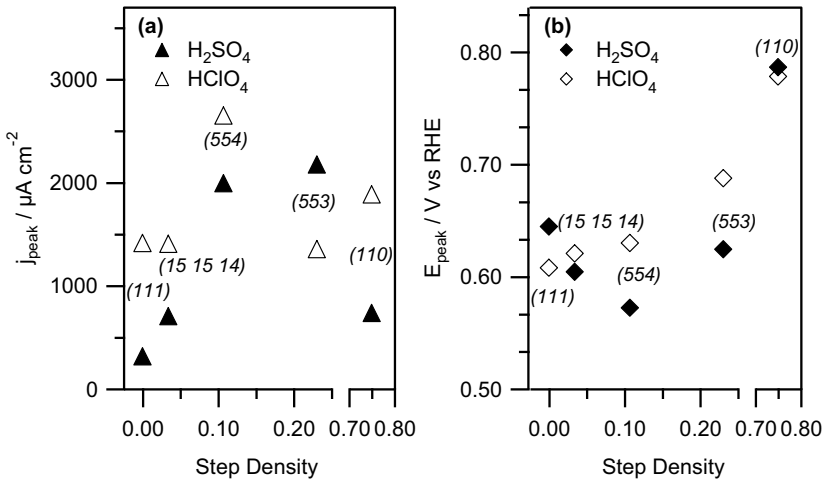

Figure 3.3: *Dependence of (a) the maximum current density and (b) the peak potential of bulk ethanol oxidation on the step density. Closed symbols denote 0.5 M H_2SO_4 as supporting electrolyte while open symbols indicate 0.1 M $HClO_4$ as supporting electrolyte.*

shifts in the peak potentials, although the trend is markedly different (Figure 3.3a). Whereas the peak potential as a function of step density shows a minimum for oxidation in sulfuric acid, in perchloric acid it is monotonously increasing with increasing step density. With the exception of Pt (553), total ethanol oxidation activities were found to be higher in perchloric acid than in sulfuric acid. The relative increase, however, is inversely related with the step density, especially on surfaces with large terraces: on Pt (111), a four-fold increase in peak current can be observed compared to sulfuric acid. As steps are introduced, this increase is reduced to about 100% for Pt (15 15 14) and 25 % for Pt (554). These results can be readily explained by the fact that (bi-)sulfate adsorption plays a larger role on surfaces with large terraces due to a preferential adsorption of (bi-)sulfate on terraces rather than on steps, in agreement with a study by Mostany *et al.* [20]. Therefore, the effect of changing the anion is larger for surfaces with wider terraces and decreases with step density. The divergence of this trend for the surfaces with a higher step density may well be the result of the markedly different interaction between (bi-)sulfate and Pt (110) compared to the interaction with (111)-terraces.

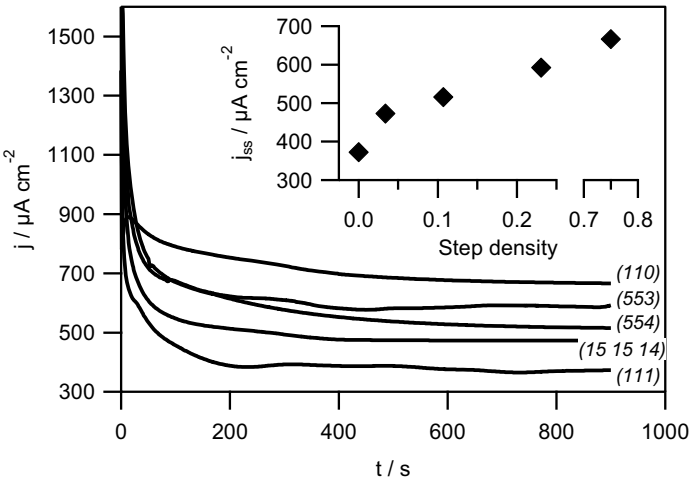

Figure 3.4: *Current-time transients for the oxidation of 0.5 M ethanol in 0.1 M $HClO_4$. The step potential was 0.7 V. The inset shows the current density after 15 minutes as a function of step density.*

Chronoamperometric measurements were also performed to study the ethanol oxidation activities over longer time-scales. The results of these experiments in perchloric acid are shown in Figure 3.4, where the potential is stepped to a value of 0.7 V, close to the maximum current in the voltammetry. On all electrode surfaces, the current shows a monotonous decay, reaching a steady state after ~3 minutes. The steady state current is positively correlated with the step density, similar to the voltammetric measurements. An important difference between the two methods, however, is the activity on Pt (110), which shows the highest activity in the chronoamperometric measurements but which has a lower activity than the stepped surfaces in the voltammetric measurements. This discrepancy could be an indication that the stepped surfaces are blocked faster by decomposition products and/or partially oxidized products than Pt (110). Although Figure 3.4 shows a marked dependence of the ethanol oxidation current on the surface structure, the qualitative effect is rather small, the maximum current between the five electrodes varying by less than a factor of two. We believe this is related to the fact that with 0.5 M ethanol, we are mainly probing the oxidation pathway to acetaldehyde [4], to be discussed in more detail in section 3.3.4.

Adsorbate stripping

In order to determine the nature of the adsorbed intermediates involved in the oxidation of ethanol, stripping experiments were conducted. In these experiments, the working electrode was introduced in a solution of 0.5 M ethanol in the supporting electrolyte under potential control and kept at this potential (E_{ad}) for 15 minutes to adsorb ethanol decomposition products. Next, the working electrode was transferred to a cell containing only the supporting electrolyte. In this cell, voltammetric sweeps in the hydrogen underpotential deposition (H_{UPD}) region, which ranges from the hydrogen evolution onset potential to roughly 0.3 V, were recorded in order to determine the amount of adsorbates (or, more precisely, the amount of sites blocked for hydrogen adsorption). After determining the total amount of adsorbates, the potential was held at 0 V for five minutes to remove all reducible adsorbates (CH_x fragments, forming methane and ethane upon reduction) [10], followed by three voltammetric sweeps up to 0.85 V to oxidize the remainder of the adsorbates (CO-like intermediates and possible remaining CH_x, forming CO_2 upon oxidation). After both the reductive and oxidative stripping processes, a cyclic voltammogram of the H_{UPD} region was recorded in order to determine the initial amounts of reducible species and oxidizable species resulting from the adsorption of ethanol in terms of H_{UPD} sites made available in the stripping process. Finally, a voltammogram was recorded at the end of the experiment and compared with a blank voltammogram recorded prior to the experiment to ascertain that a clean electrode surface is recovered by the stripping processes. With this method, it is possible to circumvent the unknown composition of the adsorbates by relating the amount of adsorbates to the amount of charge it blocks in the hydrogen adsorption area rather than quantifying it directly through evaluation of the charge involved in the stripping process, which requires the knowledge of the number of electrons needed to reduce or oxidize the ethanol decomposition products.

The results of a typical experiment as described above with Pt (553) are shown in Figure 3.5a. Curve ‘1’ shows the voltammogram of the clean surface before adsorption. Curve ‘2’ is the voltammogram of the Pt (553) electrode after ethanol chemisorption. From comparison with curve ‘1’, it is seen that the step sites are completely blocked and the terrace sites are partially blocked by

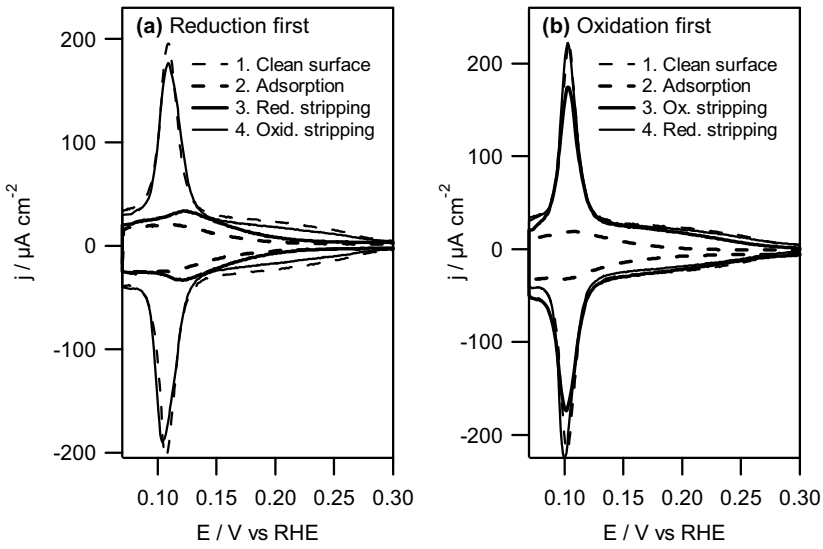

Figure 3.5: *Typical voltammetric profiles of the H_{UPD} region at various stages of the ethanol adsorbate stripping experiments on Pt (553) in 0.5 M H_2SO_4. After initial adsorption at 0.4 V, the surface was subjected to (a) reductive stripping first followed by oxidative stripping, and (b) oxidative stripping first followed by reductive stripping. The voltammograms were recorded at 50 mV s^{-1}.*

decomposition products. After reductive stripping (curve '3'), it can be seen that mostly terrace sites are made available by the stripping process, while the step sites are still blocked completely by the remaining adsorbates. The clean surface is recovered almost entirely by the following oxidative stripping (curve '4'). Figure 3.5b shows the effect of performing an oxidative rather than a reductive stripping process first after the initial adsorption. In this case, the first stripping procedure step liberates all terrace sites and part of the step sites (curve '3'). The remaining step sites are freed by the reductive stripping. Comparing Figure 3.5(a) and (b), several conclusions can be drawn. Firstly, considering the amount of sites liberated by the reductive stripping treatment in both methods, part of the CH_x-species can be removed oxidatively within a few voltammetric sweeps. This is more clearly illustrated in Figure 3.6, which shows the oxidative voltammetric sweeps of both experiments in Figure 3.5. If a reductive stripping process is performed first after the initial adsorption, the oxidative stripping

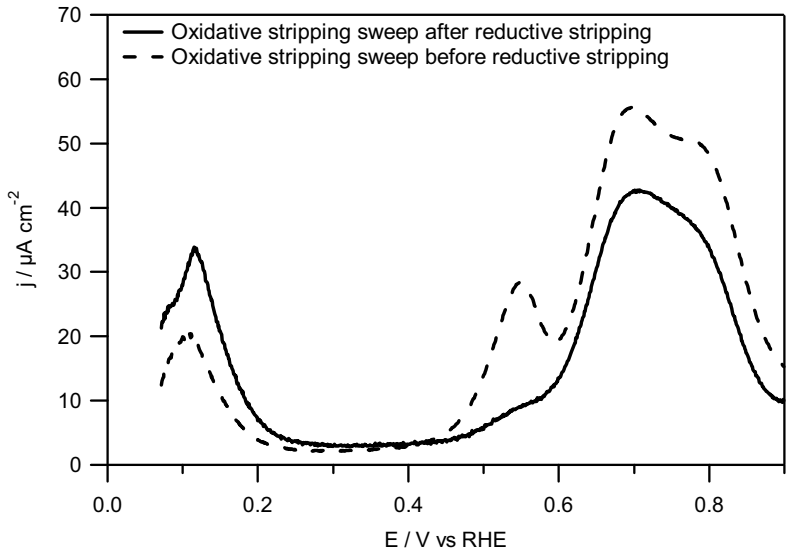

Figure 3.6: *Oxidative stripping of ethanol decomposition products at E_{ad} = 0.3 V on Pt (553) on 0.5 M H_2SO_4. The dashed line shows the stripping profile directly after adsorption, while the solid line shows the profile after the electrode surface was subjected to reductive stripping process first after the adsorption.*

sweep gives a single peak which starts at 0.5 V and has a maximum around 0.7 V. If, however, the CH_x is not removed by reduction after the initial adsorption before the oxidative stripping, an additional feature appears in the stripping voltammetric sweep around 0.5 V, with the onset at 0.4 V. In addition, the feature around 0.8 V has a larger intensity than in the case where CH_x has been removed by a reductive stripping process. Based on these findings, we tentatively attribute the feature around 0.5 V and part of the feature around 0.8 V to the oxidation of CH_x species. Most likely, the low potential feature starting at 0.4 V would signify the oxidation of $CH_{x,ad}$ to CO_{ad}, and the high potential feature to further oxidation of CO_{ad} to CO_2. This is in good agreement with results of Hahn and Melendres [21], who reported that CO_{ad} is an observed intermediate in the oxidation of methane to CO_2.

Furthermore, in both cases, the adsorbates remaining after the first stripping procedure are preferentially adsorbed at the step sites. This is especially the case when reductive stripping is applied first. This suggests that both types of

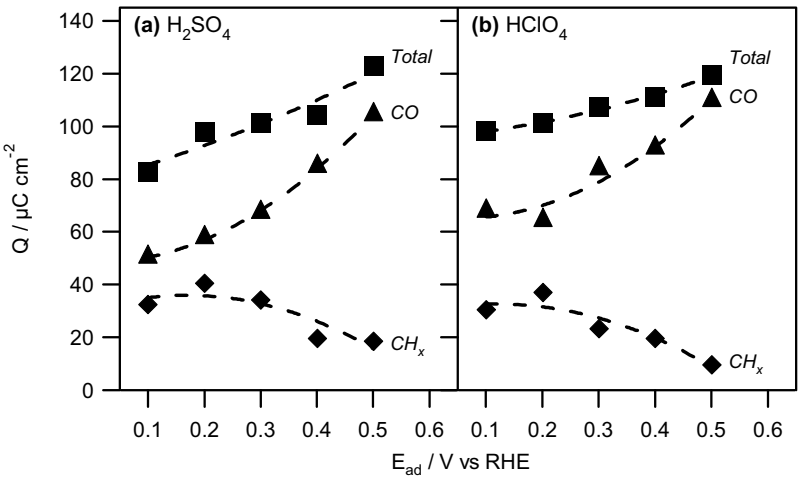

Figure 3.7: *The dependence of the amount of charge in the H_{UPD} region that is inhibited by the adsorbates resulting from ethanol decomposition on the ethanol decomposition potential on Pt (553). Triangles denote oxidizable species, while diamonds denote reducible species. Squares indicate the sum of the oxidizable and reducible species. The supporting electrolyte was (a) 0.5 M H_2SO_4 or (b) 0.1 M $HClO_4$. The dashed lines are drawn to guide the eye.*

adsorbed species have a preferential affinity for step sites as well as a significant surface mobility to migrate to the step sites once these are liberated by the removal of other adsorbates. Carbon monoxide has been known to exhibit a surface diffusion rate on platinum in acidic media [18, 22, 23]. The diffusion rates of CH_x fragments under electrochemical conditions, on the other hand, have been much less studied. An alternative interpretation of Figure 3.5 could be that CO primarily occupies the step sites, and the CH_x fragments primarily occupy the terrace sites. Comparing Figure 3.7(a) and (b), it can be seen that changing the anion of the supporting electrolyte causes little change in the stripping results. This suggests that the anion effects observed earlier in Figure 3.1 and Figure 3.2 in the electro-oxidation of ethanol are not related to the C-C bond breaking leading to adsorbed intermediates. In both media, it is clear that the total amount of adsorbates increases with increasing adsorption potential, indicating that breaking of the ethanol carbon-carbon bond and the subsequent formation of strongly adsorbed intermediates occurs to a higher degree at higher potentials.

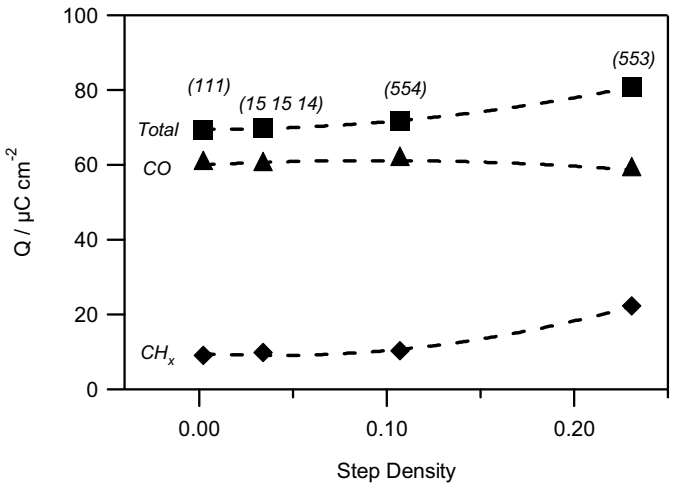

Figure 3.8: *Structure sensitivity of ethanol adsorbate stripping in 0.1 M HClO4 as implied by the amount of charge in the H_{UPD} region that is inhibited by the adsorbates. Triangles denote oxidizable species, while diamonds reducible species. Squares indicate the sum of the oxidizable and reducible species. The dashed lines are drawn to guide the eye.*

Figure 3.7 also shows that the amount of oxidizable adsorbed species increases with adsorption potential. For adsorption potentials above 0.2 V, the amounts of reducible species decreases with increasing adsorption potential. This could be due to the oxidation of the CH_x fragments to CO (or COH/CHO), which, according to Hahn and Melendres [21], may happen already at potentials as low as 0.26 V. Decreasing the adsorption potential from 0.2 V to 0.1 V, however, yields a small decrease in reducible species. Since earlier DEMS experiments [9, 10] reported the formation of small amounts of methane and ethane below 0.2 V, this finding can be attributed to the continuous reduction of the reducible species during the adsorption process.

The effect of the surface structure on the surface coverages of the different adsorbates was also investigated by employing several stepped platinum single-crystal electrodes. For these experiments, the Pt [*n*(111)×(111)] electrodes were kept at the 0.3 V for 30 minutes during the adsorption phase. The results of these experiments are shown in Figure 3.8, which reveal several interesting features. First of all, by comparing Figure 3.8 with Figure 3.7b, the total amount of adsorbed species was found to be lower when the adsorption time was increased from 15 minutes to 30 minutes. In addition, the amount of oxidizable (CO-like)

intermediates relative to reducible (CH_x) intermediates is greater for 30 minutes of adsorption than for 15 minutes of adsorption, which could indicate that slow reduction of the ethanol decomposition products already occurs during adsorption. The freed sites can accommodate new decomposition products, making the surface more and more 'CO'-rich with increasing adsorption time. An alternative explanation could be that slow conversion of CH_x to CO already occurs during the adsorption. Furthermore, although the total amount of adsorbates shows a slightly increasing trend with step density, the amount of CO-like intermediates is relatively constant over this range of surface step density. The amount of reducible intermediates, on the other hand, roughly doubles over the investigated range of step densities.

3.3.2 Acetaldehyde

Continuous oxidation

Since acetaldehyde has been reported repeatedly [4, 7, 9, 24, 25] as one of the main oxidation products of ethanol and the primary oxidation product at the 0.5 M ethanol concentration used in this work, it is clear that an improved understanding of the mechanism of acetaldehyde oxidation may assist in understanding the processes involved in the electro-oxidation of ethanol.

To this end, the oxidation of acetaldehyde was also investigated in this study. The results of the oxidation of 0.1 M acetaldehyde in 0.5 M H_2SO_4 on the different single-crystal electrodes are shown in Figure 3.9. The general shapes of the cyclic voltammograms are similar to those of the oxidation of ethanol. However, a closer inspection reveals that the currents in the positive sweep compared to the currents in the negative sweep are much lower, suggesting different electrode-reactant interactions at low potentials for ethanol and acetaldehyde. Furthermore, the results suggest that increasing the step density of the electrode surface has a smaller effect on oxidation currents than is the case for ethanol. In addition, compared to Pt (111) and the stepped surfaces, the activity of Pt (110) in acetaldehyde electro-oxidation is very low. More interestingly, the effect of increasing step density on the oxidation of acetaldehyde is opposite to that on ethanol electro-oxidation in sulfuric acid: the oxidation activity is found to decrease with increasing step density. This is more clearly shown in Figure 3.9b and c, in which the peak current and the peak

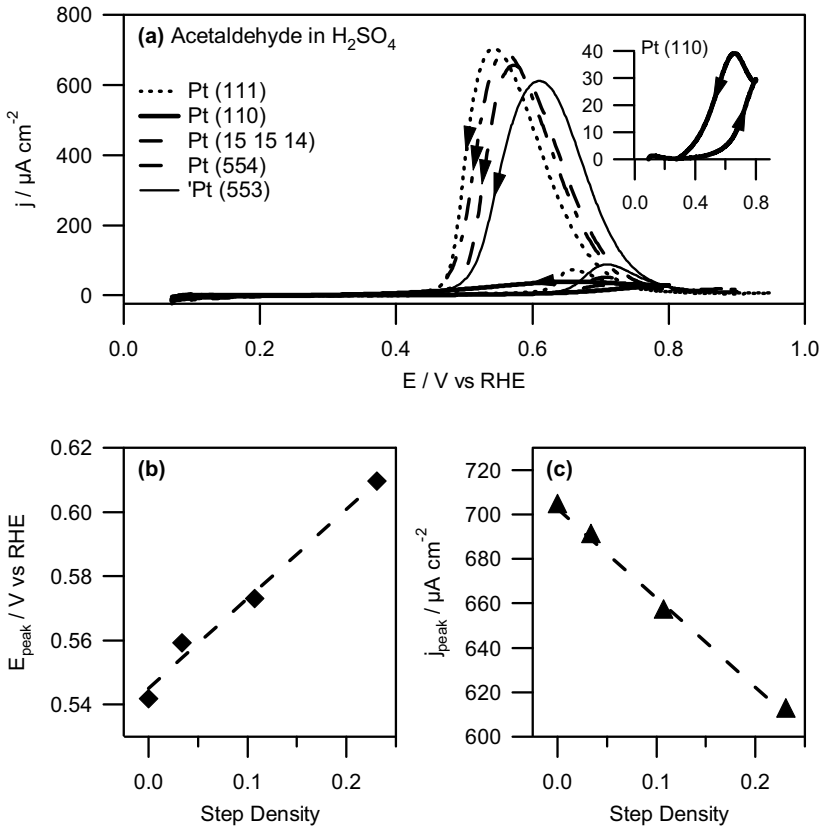

Figure 3.9: *(a) Cyclic voltammograms of the oxidation of 0.1 M acetaldehyde on platinum single-crystal electrodes in 0.5 M H_2SO_4 at a scan rate of 10 mV s^{-1}. (b) Dependence of the peak potential and (c) the maximum current density of acetaldehyde oxidation on the step density. The dashed lines are the least-squares fit of the data.*

potential, respectively, are shown as a function of step density. The correlation between both peak parameters and the step density is roughly linear, suggesting a quantitative and cumulative effect of steps in the deactivation of the oxidation of acetaldehyde.

The same experiments were also performed using perchloric acid as supporting electrolyte. Figure 3.10 shows the results of these experiments. The voltammetric profiles correspond strongly to the results employing sulfuric acid

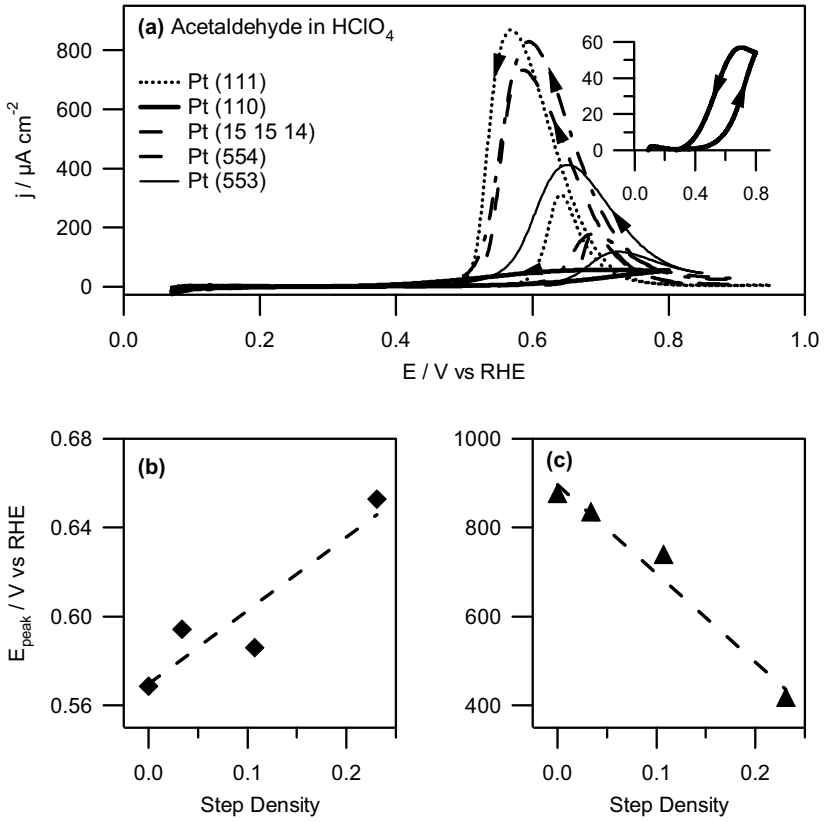

Figure 3.10: *(a) Cyclic voltammograms of the oxidation of 0.1 M acetaldehyde on platinum single-crystal electrodes in 0.1 M $HClO_4$ at a scan rate of 10 mV s^{-1}. (b) Dependence of the peak potential and (c) the maximum current density of acetaldehyde oxidation on the step density. The solid lines are the least-squares fit of the data.*

as supporting electrolyte. In general, the oxidation currents are somewhat higher in perchloric acid (again, with the notable exception of Pt (553)), although the difference is quite small. Also, as is the case for sulfuric acid electrolyte, Pt (110) is very inactive for acetaldehyde oxidation. Moreover, the negative correlation between oxidation activity and step density found for oxidation in sulfuric acid is also observed, to a greater extent, in a perchloric medium. The trend of acetaldehyde oxidation activity decreasing with step density was also confirmed in potential step measurements (Figure 3.11), at least for the stepped

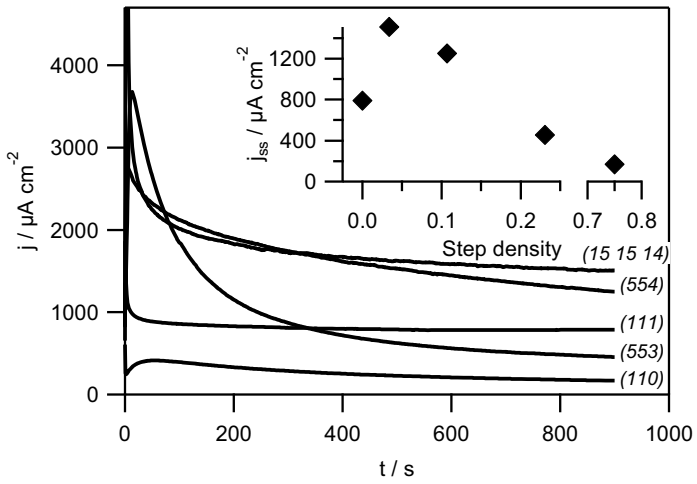

Figure 3.11: *Current-time transients of the oxidation of 0.5 M acetaldehyde in 0.1 M $HClO_4$. The step potential was 0.7 V. The inset shows the current density after 15 minutes as a function of step density.*

surfaces. The effect of the anion can again be attributed to the preferential adsorption of (bi-)sulfate on terraces rather than on steps: if acetaldehyde oxidation and (bi-)sulfate adsorption are both processes that are directly related to the number of terrace sites, it is clear that effect of switching from sulfuric acid to perchloric acid as supporting electrolyte has a larger effect on the oxidation of acetaldehyde on surfaces with wide terraces than on surfaces with narrow terraces.

Adsorbate Stripping

Stripping experiments similar to those described for ethanol were also conducted with acetaldehyde. The results of these experiments are shown in Figure 3.12. In contrast to ethanol, for acetaldehyde, increasing the adsorption potential decreases the total amount of adsorbates, although the absolute effect is rather small when using perchloric acid as supporting electrolyte. Apart from a more marked decrease of the amounts of adsorbates with adsorption potential in sulfuric acid, both electrolytes show the same behavior. From evaluating the redox behavior of the adsorbates, it can be seen that the quantity of reducible species decreases with adsorption potential in the potential range between 0.1 V

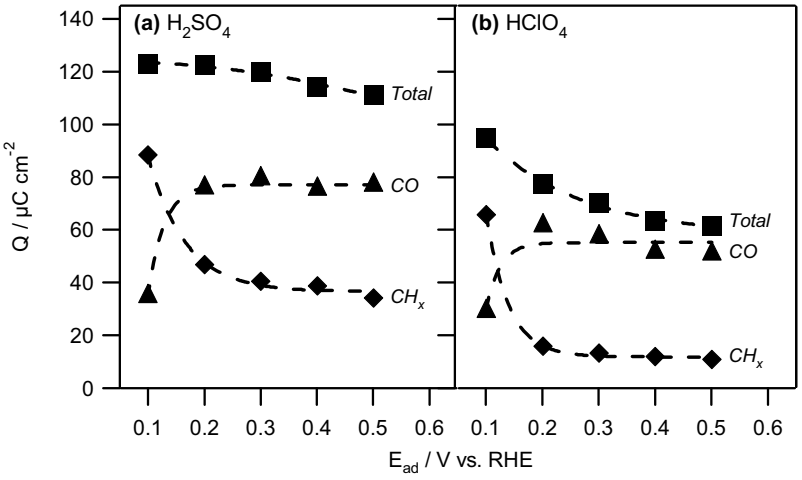

Figure 3.12: *The dependence of the amount of charge in the H_{UPD} region that is inhibited by the adsorbates resulting from acetaldehyde decomposition on the adsorption potential on Pt (553). Triangles denote oxidizable species, while diamonds denote reducible species. Squares indicate the sum of the oxidizable and reducible species. The supporting electrolyte was (a) 0.5 M H_2SO_4 or (b) 0.1 M $HClO_4$. The dashed lines are drawn to guide the eye.*

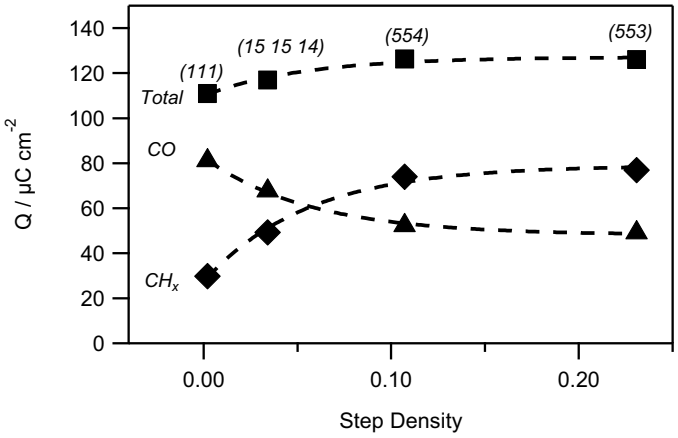

Figure 3.13: *Structure sensitivity of acetaldehyde adsorbate stripping in 0.1 M $HClO_4$ at E_{ad} = 0.3 V, as implied by the amount of charge in the H_{UPD} region that is inhibited by the adsorbates. Triangles denote oxidizable species, while diamonds denote reducible species. Squares indicate the sum of the oxidizable and reducible species. The dashed lines are drawn to guide the eye.*

and 0.5 V. Comparing this to the stripping results of the decomposition products of ethanol described earlier, where the amount of reducible adsorbates increased when the adsorption potential was increased from 0.1 V to 0.2 V, this would imply that the reducible adsorbates resulting from ethanol adsorption are easier to reduce than those resulting from acetaldehyde adsorption. The amounts of oxidizable species increase strongly by stepping the adsorption potential from 0.1 V to 0.2 V, after which it remains essentially constant for adsorption potentials up to 0.5 V.

Results of acetaldehyde adsorbate stripping on different surfaces are shown in Figure 3.13. For these experiments, acetaldehyde was adsorbed on the different platinum single-crystal electrodes at 0.3 V for 30 minutes. It can be seen that, similar to ethanol, the total amount of adsorbates increases with step density, indicating that step sites catalyze the carbon-carbon bond breaking. In addition, the composition of the adsorbates is strongly dependent on the surface structure: increasing the step density decreases the amount of oxidizable species while increasing the amounts of reducible species.

3.3.3 Acetic acid

Voltammetric profiles of acetic acid on Pt (111) in different electrolytes are shown in Figure 3.14. It can be seen that, although the blank voltammetry of a well-ordered Pt (111) electrode shows large differences depending on the nature of the electrolyte, no significant differences are observed in the cyclic voltammograms recorded in 0.1 M acetic acid in all solutions. For all electrolytes, there is no oxidation activity within the potential range of interest. Furthermore, the voltammetric behavior of acetic acid on Pt (111) in all electrolytes is very comparable to that of sulfuric acid. Similar results were found for the other electrodes of the Pt [*n*(111)×(111)] - series studied in this work. Since the voltammetric profile of acetic acid closely mirrors that of sulfuric acid, or, more generally, of (bi-)sulfate species in the electrolyte solution, the voltammetric behavior of acetic acid can be considered in an analogous manner. The potential region between 0.0 V and roughly 0.3 V can be described as the hydrogen underpotential region. Starting at 0.3 V, a broad feature can be seen extending up to 0.8 - 0.9 V. The charge density derived from

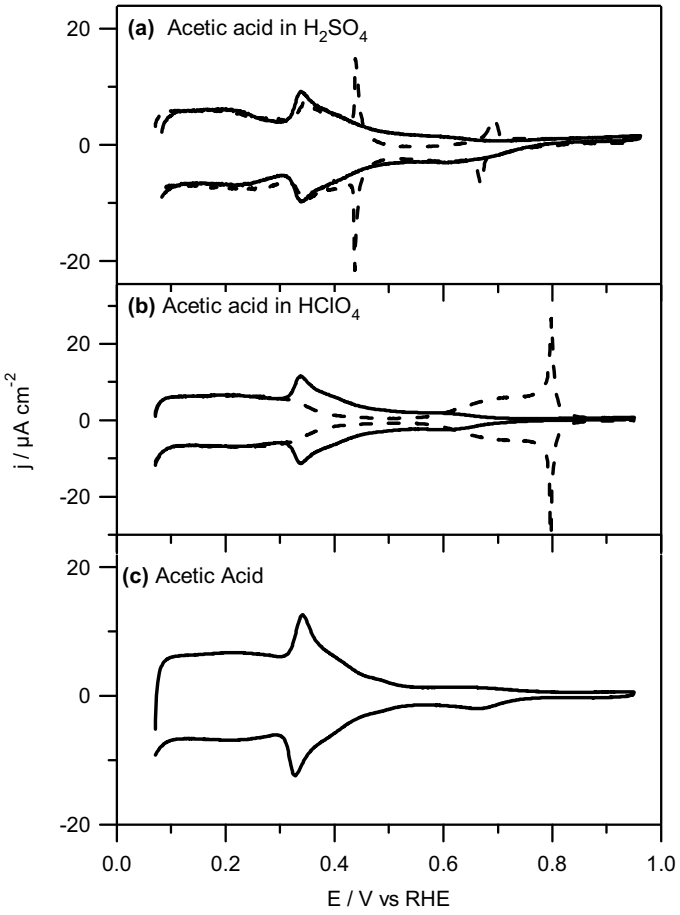

Figure 3.14: *Voltammetric profiles of 0.1 M acetic acid on Pt (111) in (a) 0.5 M H_2SO_4 (b) 0.1 M $HClO_4$ and (c) water. The dashed lines represent the voltammograms recorded in blank supporting electrolyte. The scan rates were 10 mV s^{-1}.*

this feature was 100 ± 4 µC cm^{-2} for all electrolytes, which is somewhat higher than the charge density for the (bi-)sulfate adsorption, which is around 80-90 µC cm^{-2} [15, 26]. The charge involved in this feature can be ascribed to the adsorption of acetic acid, most likely as acetate, and correspond to a coverage of 0.41 ± 0.02 monolayers. The fact that the presence of the specifically adsorbing (bi-)sulfate does not significantly alter the charge involved in the adsorption of acetic acid, indicates that acetic acid adsorbs more strongly than (bi-)sulfate.

Figure 3.14 clearly shows that the formation of acetic acid should be considered a 'dead end' in the ethanol oxidation scheme.

3.4 General Discussion

Based on the results presented here, as well as previously published studies, we propose a mechanism for the electrochemical oxidation of ethanol as shown in Scheme 3.1. This scheme includes the formation of strongly adsorbed intermediates and the formation and oxidation of acetaldehyde, as well as the non-reactivity of acetic acid. Scheme 3.1 is similar to the reaction scheme proposed by Tremiliosi-Filho *et al*. for the oxidation of ethanol on gold [27], with the difference that that scheme does not include C-C bond breaking. Our scheme relies heavily on the results obtained in ultra-high vacuum (UHV) that the C-C bond primarily breaks after dehydrogenation to acetaldehyde [28, 29]. Theoretical [30] and ultra-high vacuum (UHV) [29] studies suggest that, initially, ethanol adsorbs weakly to the platinum surface through the lone pair electrons on the oxygen (reaction 1). Once adsorbed, ethanol can be oxidized to (weakly) adsorbed acetaldehyde, a reaction requiring two dehydrogenation steps (reaction 2). In UHV, the first dehydrogenation step is the cleavage of the O-H bond, giving rise to an adsorbed ethoxy [29], but under electrochemical conditions it has been suggested that the first bond to be broken is the α-C-H bond [8, 31]. Since, for the ethanol concentration investigated in this study, DEMS measurements have shown that the main ethanol oxidation product is acetaldehyde [4], it can be safely assumed that the measurements shown in Figure 3.1, Figure 3.2 and Figure 3.4 mainly show the current arising from the conversion of ethanol to acetaldehyde. Due to the relatively small anion effect illustrated in Figure 3.3 and a small but significant effect of surface structure, it can be concluded that the oxidation of ethanol to acetaldehyde is a surface sensitive process, occurring preferentially at or near step sites on the electrode.

Since strongly adsorbed species are observed after adsorbing ethanol at potentials as low as 0.1 V, while no significant oxidation currents for ethanol are observed below 0.3 V in this study, we cannot exclude a direct pathway from adsorbed ethanol to decompose into adsorbed CH_x and adsorbed CO (reaction 3). At the same time, acetaldehyde can also decompose into these species at

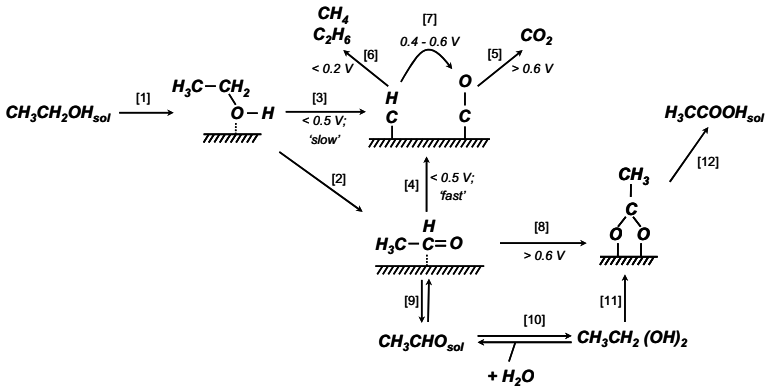

Scheme 3.1: *Schematic representation of a suggested mechanism of the electrochemical oxidation of ethanol on platinum electrodes at the high concentrations of ethanol used in this study.*

these low potentials (reaction 4) [11]. Comparing Figure 3.8 and Figure 3.13, it can be seen that the total coverage resulting from acetaldehyde decomposition is higher than that from ethanol decomposition, indicating that carbon-carbon bond breaking occurs to a greater extent in acetaldehyde. This is supported by most UHV studies [28, 29], which, as mentioned, often indicate acetaldehyde as a necessary intermediate in the decomposition of ethanol. On the other hand, a study by Cong and coworkers [28] hints indirectly at the ethanolic carbon-carbon bond partially being broken before the formation of acetaldehyde, especially at the (110) step sites on a Pt (331) surface. Therefore, we suggest that the main species in which the ethanol carbon-carbon bond is broken is acetaldehyde, especially in the potential range in which ethanol is readily oxidized to acetaldehyde. However, at low potentials (< 0.3 V), C-C bond breaking may occur in ethanol or ethoxy, especially at step sites, in agreement with the suggestion made by Cong *et al* [28]. CO resulting from the ethanol and acetaldehyde decomposition can be oxidized at potentials above *ca.* 0.5 V (reaction 5). The adsorbed hydrocarbon fragment can be removed completely by reduction below 0.1 V (reaction 6). Our stripping results suggest that the adsorbed CH_x fragments may be oxidized to CO_{ad} at 0.4 V and subsequently to CO_2 at somewhat higher potential, and that therefore they are not more poisoning that adsorbed CO.

Apart from decomposition to yield strongly adsorbed carbon containing species, acetaldehyde can be further oxidized without the breaking of the C-C bond to yield acetic acid (acetate). Relatively little is known about the pathway in which acetic acid is generated. It has been suggested that acetaldehyde can react directly with a surface oxygenated species [11], such as OH_{ad} into adsorbed acetate (reaction 8). Alternatively, since acetaldehyde is readily hydrolyzed to in an aqueous environment, acetic acid can be formed by the oxidation of the resulting geminal diol (reactions 9 - 12) [32], similar to the suggested oxidation mechanism of ethanol on gold [27] and of formaldehyde on platinum to formic acid [19].

With Scheme 3.1 in mind and by combining the results of the adsorbate stripping experiments with the results of bulk oxidation experiments, we propose the following hypothesis for the seemingly (counter-intuitive) behavior of the effect of steps on the electro-oxidation activity for ethanol and acetaldehyde. For ethanol oxidation at a high ethanol concentration, the current is mainly the result of the oxidation of ethanol to acetaldehyde (reaction 2). This reaction has a (small) preference for step sites. Since direct C-C breaking in ethanol or ethoxy (reaction 3) is sluggish, and the concentration of acetaldehyde is still too low to lead to step poisoning, the overall activity increases with rapid step density. For acetaldehyde, the current is mainly due to the reaction of acetaldehyde to acetic acid (reactions 8 - 12) at potentials above 0.7 V [11]. However, C-C bond breaking in acetaldehyde (reaction 4) is fast, and therefore, step sites are rapidly blocked. If reaction 8 or reaction 11 prefers step sites, this would explain a decreasing overall activity with step density.

A remaining puzzling feature is the different stability of the CH_x fragments from ethanol and acetaldehyde, those from ethanol apparently being less stable, especially at low potentials (compare Figure 3.7 and Figure 3.12). This may be related to the oxidizability of the CH_x fragments, as Hahn and Melendres have reported the possibility of oxidizing methane adsorbates on platinum to COH_x fragments at potentials close to or in the hydrogen region.

3.5 Conclusions

In this chapter, we have presented the results of a systematic electrochemical study of the oxidation of ethanol and acetaldehyde on well-defined platinum

single-crystal surfaces for high concentrations of ethanol and acetaldehyde in solution. For ethanol, it was found that the continuous oxidation show a significant degree of surface sensitivity, with the total oxidation activity in general increasing with the concentration of defect sites (steps). In the case of acetaldehyde, however, this finding is reversed. To elucidate the effect of the surface structure on the breaking of the carbon-carbon bond, adsorbate stripping experiments were performed both with ethanol and acetaldehyde. Our results suggest that the C-C bond breaking occurs preferentially in acetaldehyde, suggesting that acetaldehyde is the main species in which the bond is broken in the ethanol reaction mechanism although slow C-C bond breaking in ethanol and ethoxy cannot be excluded. Finally, based on our results and the existing literature, a detailed scheme of the ethanol oxidation mechanism was presented, which incorporates the formation of carbon dioxide, acetaldehyde and acetic acid, products of the electrochemical oxidation of ethanol, as well as the formation of adsorbed intermediates detected by spectroscopic methods. Based on this mechanism, we suggest that step poisoning is slow for ethanol oxidation, leading to a positive effect of the step density on the conversion of ethanol to acetaldehyde. On the other hand, the step poisoning is rapid for acetaldehyde because of the relative ease of C-C bond breaking, leading to an adverse effect of steps on the oxidation of acetaldehyde to acetic acid.

3.6 References

1. D. J. Tarnowski and C. Korzeniewski, *J. Phys. Chem. B*, **1997**, *101*, 253-258.
2. J. Shin, W. J. Tornquist, C. Korzeniewski and C. S. Hoaglund, *Surf. Sci.*, **1996**, *364*, 122-130.
3. F. Vigier, C. Coutanceau, F. Hahn, E. M. Belgsir and C. Lamy, *J. Electroanal. Chem.*, **2004**, *563*, 81-89.
4. G. A. Camara and T. Iwasita, *J. Electroanal. Chem.*, **2005**, *578*, 315-321.
5. T. Iwasita and E. Pastor, *Electrochim. Acta*, **1994**, *39*, 531-537.
6. J. T. Wang, S. Wasmus and R. F. Savinell, *J. Electrochem. Soc.*, **1995**, *142*, 4218-4224.
7. S. C. Chang, L. W. H. Leung and M. J. Weaver, *J. Phys. Chem.*, **1990**, *94*, 6013-6021.

8. J. Willsau and J. Heitbaum, *J. Electroanal. Chem.*, **1985**, *194*, 27-35.
9. H. Wang, Z. Jusys and R. J. Behm, *J. Phys. Chem. B*, **2004**, *108*, 19413-19424.
10. U. Schmiemann, U. Muller and H. Baltruschat, *Electrochim. Acta*, **1995**, *40*, 99-107.
11. M. J. S. Farias, G. A. Camara, A. A. Tanaka and T. Iwasita, *J. Electroanal. Chem.*, **2007**, *600*, 236-242.
12. J. Clavilier, D. Armand, S. G. Sun and M. Petit, *J. Electroanal. Chem.*, **1986**, *205*, 267-277.
13. J. Clavilier, K. El Achi and A. Rodes, *Chem. Phys.*, **1990**, *141*, 1-14.
14. N. P. Lebedeva, M. T. M. Koper, J. M. Feliu and R. A. van Santen, *Electrochem. Commun.*, **2000**, *2*, 487-490.
15. A. M. Funtikov, U. Stimming and R. Vogel, *J. Electroanal. Chem.*, **1997**, *428*, 147-153.
16. C. G. M. Hermse, A. P. van Bavel, M. T. M. Koper, J. J. Lukkien, R. A. van Santen and A. P. J. Jansen, *Surf. Sci.*, **2004**, *572*, 247-260.
17. N. P. Lebedeva, M. T. M. Koper, E. Herrero, J. M. Feliu and R. A. van Santen, *J. Electroanal. Chem.*, **2000**, *487*, 37-44.
18. N. P. Lebedeva, M. T. M. Koper, J. M. Feliu and R. A. van Santen, *J. Phys. Chem. B*, **2002**, *106*, 12938-12947.
19. T. H. M. Housmans, A. H. Wonders and M. T. M. Koper, *J. Phys. Chem. B*, **2006**, *110*, 10021-10031.
20. J. Mostany, E. Herrero, J. M. Feliu and J. Lipkowski, *J. Phys. Chem. B*, **2002**, *106*, 12787-12796.
21. F. Hahn and C. A. Melendres, *Electrochim. Acta*, **2001**, *46*, 3525-3534.
22. M. Bergelin, E. Herrero, J. M. Feliu and M. Wasberg, *J. Electroanal. Chem.*, **1999**, *467*, 74-84.
23. W. Akemann, K. A. Friedrich and U. Stimming, *J. Chem. Phys.*, **2000**, *113*, 6864-6874.
24. J. F. Gomes, B. Busson and A. Tadjeddine, *J. Phys. Chem. B*, **2006**, *110*, 5508-5514.
25. X. H. Xia, H. D. Liess and T. Iwasita, *J. Electroanal. Chem.*, **1997**, *437*, 233-240.
26. A. Kolics and A. Wieckowski, *J. Phys. Chem. B*, **2001**, *105*, 2588-2595.
27. G. Tremiliosi-Filho, E. R. Gonzalez, A. J. Motheo, E. M. Belgsir, J. M. Leger and C. Lamy, *J. Electroanal. Chem.*, **1998**, *444*, 31-39.

28. Y. Cong, V. van Spaendonk and R. I. Masel, *Surf. Sci.*, **1997**, *385*, 246-258.
29. A. F. Lee, D. E. Gawthrope, N. J. Hart and K. Wilson, *Surf. Sci.*, **2004**, *548*, 200-208.
30. R. Alcala, M. Mavrikakis and J. A. Dumesic, *J. Catal.*, **2003**, *218*, 178-190.
31. E. Sokolova, *Electrochim. Acta*, **1975**, *20*, 323-330.
32. R. P. Bell and B. D. Darwent, *Trans. Far. Soc.*, **1950**, *46*, 34-41.